INDIAN JOURNAL OF SCIENCE AND TECHNOLOGY

RESEARCH ARTICLE

Analyzing Color Features to Realize Adaptive Contour Model for Segmentation

Ramya Srikanteswara[1]*, **A C Ramachandra**[2]

1 Assistant Professor, Department of CS&E, Nitte Meenakshi Institute of Technology, Bengaluru, Karnataka, India
2 Professor & Head, Department of ECE, Nitte Meenakshi Institute Of Technology, Bengaluru, Karnataka, India

OPEN ACCESS

Received: 19-05-2023
Accepted: 27-09-2023
Published: 15-12-2023

Citation: Srikanteswara R, Ramachandra AC (2023) Analyzing Color Features to Realize Adaptive Contour Model for Segmentation . Indian Journal of Science and Technology 16(46): 4378-4387. https://doi.org/10.17485/IJST/v16i46.1215

* **Corresponding author**.

ramya.srikanteswara@nmit.ac.in

Funding: None

Competing Interests: None

Published By Indian Society for Education and Environment (iSee)

ISSN
Print: 0974-6846
Electronic: 0974-5645

Abstract

Background/Objectives: Melanoma cases have taken a sharp rise in recent years all across the world which is the reason of concern for many health institutions and the most concerning subject for many medical experts is its high mortality rate which causes thousands of lives every year. The main objective is to develop and evaluate a new system which can detect melanoma at an earlier stage. **Methods:** An efficient lesion segmentation method is introduced for the detection of Melanoma skin cancer disease at the preliminary stages using Adaptive Contour Model (ACM). The dataset used here is PH2 and ISIC Challenge 2017 Dataset images. 800 images are considered for the testing. High-quality segmentation is achieved based on contour features and sharp edge detection using ACM. An image is segregated into two set functions to analyze PH2 and ISIC Challenge 2017 Dataset images. **Findings:** The performance of the proposed Adaptive Contour Model (ACM) is tested upon PH2 and ISIC Challenge 2017 Dataset. The Performance matrices for the segmentation process are *Jaccard* index (JA) is 79.23, the Dice coefficient (DI) is 87.26, and the accuracy (AC) is 94.63 considering ISIC dataset. The performance indices are such as *Jaccard* index (JA) is 89.14, the Dice coefficient (DI) is 93.98, and the accuracy (AC) is 96.95 which is quite high considering PH2 dataset. **Novelty:** A method for detection of melanoma has been the critical need of the day. There are various findings available for segmentation of a medical image. However, there is a need for a method where it is applicable when the threshold based method may not be effective. This proposed method shows that the performance of the Active Contour Model (ACM) is more than 95%, which is better than other methods which lie around 92 to 94 percent.

Keywords: Contour Features; Adaptive Contour Model; Lesion Segmentation; Melanoma; Dermoscopic Images

1 Introduction

Recently, the number of skin cancer cases has taken drastic growth all over the world due to high global warming. Thus, the significance of research on skin cancer detection is extremely high for various medical reasons. Skin cancer is one of the rapidly emergent cancer in all cancer types whose mortality rate is extremely high. Melanoma skin cancer disease is one of the most dangerous forms of skin cancer disease with the highest mortality rate in all kinds of skin cancer diseases. Melanoma consists of malignant tumour which grows due to pigment present in the cells named as 'melanocytes'. The survival possibility of skin cancer patients is extremely low in later stages. According to research conducted in the United States of America (USA), every year 90 thousand new cases of patients are diagnosed with skin cancer disease in the USA [(1)]. The diagnosis of skin cancer disease is an extremely challenging procedure for medical experts and doctors, especially in advanced stages. However, early identification of skin cancer disease and timely diagnosis of this disease can provide extremely positive results. Skin cancer disease can be diagnosed proficiently using the methods like "ABCD rule "and "7-point checklist" etc. Skin cancer disease can be of various types. However, Melanoma skin cancer disease is extremely fatal, rapidly spreadable, and most challenging in terms of diagnosis in all skin cancer types.

According to a study conducted by the American Cancer Disease Society, around 1 lakh cases are identified with Melanoma skin cancer disease in the USA in 2019. There are several techniques which can detect the presence of skin cancer. Here the main concern is the time taken. If the time taken is more, it may prove fatal [(2)]. Few techniques used to detect have proved to be accurate. The need of the hour is to detect melanoma in early stage. Few methods deal with a particular data type, whereas the dataset proposed here is quite vast. Around 800 images with varying colour, border and texture have been tested. Few advanced algorithms have been used to cover the gap that exists. Few existing methods were surveyed to understand the existing methods and to overcome their drawbacks

The early identification of Melanoma skin cancer disease is an extremely challenging process. Various methods can be utilized for the identification of Melanoma detection such as clinical trials, *dermoscopic* image analyzation, visual screening, biopsy etc. Melanoma disease mainly comes with a black or brown color but can be transformed into blue, slight purple, or skin-type color. In traditional methods the patient had to visit an experienced dermatologist. Due to advanced methods the diagnosis has become faster, which can lead to reduced death rate [(3)]. The main steps involved are image acquisition, preprocessing to remove noise, segmentation, followed by extraction and classification. The most extensively used traditional method used was ABCD method, which considered asymmetry, border, colour and diameter of the affected area [(4)]. Therefore, the Lesion segmentation of these *Dermoscopic* high-resolution images is the fundamental phase in the proficient diagnosis of Melanoma disease. The significance of the segmentation process is extremely high in medical applications for treatment management and disease analysis. However, the lesion segmentation procedure is a highly critical process due to the presence of different textures, structures, patterns, colors, sizes and lesion positions in these *Dermoscopic* images. The additional influencers such as hairs, air bubbles, blood vessels and lightning color can make segmentation process even more critical and challenging for medical experts. Therefore, several researchers have shown their interest in this area by providing various segmentation techniques to identify melanoma disease in its initial stages.

Few Recent literature works in image segmentation is discussed here.

In [(5)], a whale optimization process is adopted for effective lesion segmentation of the *Dermoscopic* images over the cloud based on encrypted privacy-preserving architecture. Segmentation of images is obtained in this method by segregating the encrypted images into clusters and a unique centroid is represented for every pixel of encrypted image. In [(6)], an efficient image segmentation of *Dermoscopic* images is achieved based on the two algorithms such as *GrabCut* and You Only Look Once (YOLO). This method is tested upon PH2 as well as ISIC Challenge 2017 dataset. In [(7)], an automated lesion segmentation method is presented based on the mutual bootstrapping architecture. Deep neural networks are utilized for effective classification of *Dermoscopic* images. This technique addresses the problems of dice loss and rank loss in classification process that is caused due to class and pixel imbalance. However, the significance of classification in segmentation process is not discussed comprehensively. The above literature states that there have been several research works are contributed towards Melanoma segmentation process. However, only few techniques are implemented in practice and various segmentation issues faced by medical experts in real time practice such as $artifacts$, fuzzy boundary issues, lesion position identification issue, lesion pixel and neighbouring skin area imbalance problem, pixel overlapping problem, presence of intrinsic features like hairs, blood vessels etc. These factors make segmentation process challenging and complex. Therefore, a proficient technique is required for proper lesion segmentation and removal of $artifacts$ in the *Dermoscopic* images.

Skin cancer cases have emerged with its full potential in recent years which has enhanced the significance of skin disease identification in preliminary stages. Moreover, Melanoma skin cancer disease is the most concerning all skin cancer types due to its high death rate. Therefore, various researchers have suggested that comprehensive study of *Dermoscopic* image lesions can prove to be a very significant process to deal with Melanoma disease. However, study of *Dermoscopic* images directly

depends upon three crucial aspects like segmentation, feature extraction and feature classification. Here, Segmentation is the preliminary stage to understand *Dermoscopic* image lesions and for the identification of Melanoma cancer disease. Therefore, several researchers have focused their attention to Melanoma disease analysis. Some of the recent researches has been presented in following paragraph.

In[8], a skin lesion segmentation technique is introduced with the help of *DenseUnet Network* in coordination with attention-based Adversarial Training. *DenseUnet Network* Architecture is utilized to ensure maximum information extraction from multiple layers of *Dermoscopic* images. This model is evaluated upon ISIC Challenge 2017 dataset. In[9], skin cancer diagnose technique is adopted with the help of Melanoma and Nevus classification process of medical images. Gaussian filter is utilized for mitigating noise from digital images. The performance of this model is evaluated upon DERMIS dataset. In[10], deep learning techniques are introduced for the segmentation of Melanoma *Dermoscopic* images. The main focus of this article is efficient lesion boundary segmentation. Various lesion types are detected using this technique. This model is tested upon PH2 as well as ISIC Challenge 2017 dataset. In[11], a skin lesion segmentation technique is presented based on the feature learning and decision fusion. Bi-directional feature learning architecture is adopted to evaluate critical correlation coefficient between images. Convolutional Neural Network (CNN) is utilized for improvement of passing efficiency. Decision fusion is used to explain consistency of decision at every position. In[12], an automated Melanoma identification model has been adopted based on the deep learning techniques. For enhancement in the efficiency of feature extraction, an encoder-decoder model is introduced. Pixel-wise classification is conducted on *Dermoscopic* images. In[13], a deep learning framework is presented for the automation of skin cancer identification using *Dermoscopic* images. Here, fine-grained features are extracted using Lightweight CNN architecture. The performance of this model is evaluated upon ISIC Challenge 2016 dataset. In[14], a skin lesion segmentation technique is introduced which works in coordination with Patch-based CNN architecture. This model mitigates the class imbalance issues identified in classification process. For ground truth annotation a loss weighted strategy is adopted. The performance is tested upon SPC dataset using this technique. In[15], an automated lesion segmentation technique is introduced and lesion shape, diameter, color symmetry of *Dermoscopic* images is evaluated. A decision tree classifier is adopted for evaluation of color symmetry between images. Color features are extracted using this model. In[16] One of the major challenge in the field of medical image processing, which is uneven surface illumination and nonuniform intensity, which are triggered by the site of a convex surface or light source is addressed. The paper addresses the issue in three main stages. Firstly, it finds the Pre-fitting reflectance, secondly reconstruction in the image domain takes place, Finally the difference between low-frequency component to approximate the reflectance and the global domain are noted. In[17] the author considers the image segmentation, where the author has used edge based information. The inputs are vector based region and edge information, that can be applied to multi-modal images, multi-channel images efficiently. The proposed method uses Edge based and Contour based methods.

The above mentioned literature presents various techniques for efficient segmentation of Melanoma and Non-Melanoma images. However, several experts have issues in real-time implementation of these techniques and various issues are identified by several researchers while segmentation of Melanoma disease on *Dermoscopic* images. Some of the issues are presence of *artic facts*, texture identification, color symmetry issues, unknown lesion sizes as well as their positions and intrinsic features like hairs, blood vessels etc. Therefore, to counter these issues and for the detection of Melanoma in preliminary stages an efficient lesion segmentation method is realized based on Adaptive Contour Model (ACM) and timely comprehensive assessment of Melanoma disease is also discussed.

2 Methodology

Melanoma is one of the most dangerous skin cancer among all the possible skin cancer diseases. However, melanoma can be treated efficiently if identified in the initial stages. Thus, Image segmentation is quite important for the early detection of skin cancer diseases. There are some classical segmentation models that have been already presented by various researchers. However, segmentation is quite a challenging process due to the availability of a few artifacts like pixel overlapping problems, and the presence of intrinsic features like hairs, blood vessels, etc. Therefore, the proposed Adaptive Contour Model (ACM) is adopted to analyse dermoscopic images and get high segmentation accuracy, and segment proper boundaries with accurate edges.

An efficient lesion segmentation method is realized for the detection of Melanoma skin cancer disease at preliminary stages and timely comprehensive assessment of Melanoma disease based on Adaptive Contour Model (ACM). The proposed Adaptive Contour Model can be effectively utilized to manage heterogeneous entities with the help of Gaussian prototypes. The proposed AC model extracts contour features from the *Dermoscopic* image lesions in coordination with Gaussian structures. The proposed AC model extract contour features of various classes adaptively due to which color pixels of *Dermoscopic* image lesions can be varied. *Artifacts* Present in the *Dermoscopic* image can be mitigated using the proposed AC model along with

pre-processing strategies.

A comprehensive mathematical representation of proposed Adaptive Contour model is presented in this article. The datasets used for testing are PH2 and International Skin Imaging Collaboration (ISIC) Challenge 2017 Dataset. Both the datasets consists of *Dermoscopic* images and their respective Ground Truth (GT) images. Moreover, PH2 dataset contains 200 *Dermoscopic* melanocytic lesions for testing. The size of all PH2 *Dermoscopic* images is 768 $\times$ 560. This dataset covers three main disease types such as normal nevus, unusual nevus and Melanoma in the ratio of 80 : 80 : 40 images respectively. Similarly, ISIC Challenge 2017 Dataset contains total number of 2000 *Dermoscopic* images. All the 2000 *Dermoscopic* images are utilized for training, then, 600 *Dermoscopic* images are taken for testing and 150 images are utilized for validation purpose. The resolution of all ISIC 2017 *Dermoscopic* images changes from 4499 $\times$ 6748 to 540 $\times$ 722 pixels. Moreover, ISIC challenge 2017 dataset contains 1372 normal nevus images, 254 keratosis images and 374 Melanoma images. Based on visual efficiency and comparison with various state-of-art-techniques in terms of different evaluation parameters such as accuracy, specificity, *Jaccard Index* and Dice coefficient. The proposed Adaptive Contour Model (ACM) provides satisfactory results for the segmentation process.

2.1 Contour Feature Extraction using Adaptive Contour Model (ACM)

Several researchers have made their efforts in bringing down the mortality rate of Melanoma cases. The foremost phase to achieve this is a comprehensive study of *Dermoscopic* images, their patterns, structures, lesion sizes, positions etc. However, Image Segmentation, Feature extraction and Feature Classification have the direct impact on *Dermoscopic* image analysis. Therefore, Segmentation of *Dermoscopic* images is one of the most significant and critical phase in Melanoma disease detection. Thus, a comprehensive mathematical modelling for segmentation of *Dermoscopic* images based on the proposed Adaptive Contour Model (ACM) is presented in the following section

Assume that the input *Dermoscopic* image fed to the proposed Active Contour Model (ACM) can be represented as $M(y):\ \lambda \to Z$ where λ is a subset of a set Z^G and λ can be described as spatial field of an image. The boundary function for the sub-domains of an image can be described by a function $v(y):\ \lambda \to Z$ where v changes across the boundary of sub-domains. Similarly, the Contour function for a *Dermoscopic* image can be expressed as $P(h):\ Z \to \lambda$ to analyse edges of the sub-domain. Then the energy distribution function can be represented by the following equation,

$$S(v,P) = \int_{\lambda} (M-v)^2 . dx + \Omega \int_{\frac{\lambda}{P}} |\nabla v|^2 . dx + w|P| \tag{1}$$

Where, Ω and w are the two constants which remain positive and Contour size can be expressed as $|P|$. An efficient segmentation of a *Dermoscopic* image can be obtained by minimizing energy distribution function shown in the Equation (1) with corresponds to $|P|$ and $|v|$. Equation (1) can be minimized by considering two set functions such as $\lambda_{in(P)} \bigcup \lambda_{out(P)} = \lambda$ and $\lambda_{in(P)} \bigcap \lambda_{out(P)} = \Phi$ where the image fields λ can be disengaged by Contour P. An image is segregated into different image fields and for every image field two set functions can be utilized. Then, the energy distribution function can be simplified using the proposed Adaptive Contour Model (ACM) by the following function as,

$$S(f_1, f_2, P) = \int_{in(P)} (M-f_1)^2 . dx + \int_{out(P)} (M-f_1)^2 . dx + w|P| \tag{2}$$

Where, the constant parameters f_1 and f_2 are utilized to estimate the color pixel present inside and outside of a Contour P correspondingly. Further simplification of energy distribution function in Equation (2) provides the energy minimization function. Hence, the set function $\Theta(y):\ \lambda \to Z$ represents the Contour function $P(h):\ Z \to \lambda$ as,

$$P = [y \in \lambda \ | \Theta(y) = 0] \tag{3}$$

Then, the *Dermoscopic* image can be estimated with the help of two boundary functions $v^+(y)$ and $v^-(y)$. Here, image fields for corresponding two boundary functions $v^+(y)$ and $v^-(y)$ can be represented as,

$$P^+ = [y \in \lambda \ | \Theta(y) \succ 0] \tag{4}$$

$$P^- = [y \in \lambda \ | \Theta(y) \prec 0] \tag{5}$$

Then, the energy minimization function using the proposed Adaptive Contour Model can be represented as,

$$\begin{aligned} S(v^+, v^-, \Theta) = & \int_{\lambda} (v^+ - M)^2 (\mathbb{R}(\Theta)) . dx + \Omega \int_{\lambda} |\nabla v^+|^2 (\mathbb{R}(\Theta)) . dx \\ & + \int_{\lambda} (v^- - M)^2 (1 - \mathbb{R}(\Theta)) . dx + \Omega \int_{\lambda} |\nabla v^-|^2 (1 - \mathbb{R}(\Theta)) . dx \\ & + w \int_{\lambda} |\nabla \mathbb{R}(\Theta)| . dx \end{aligned} \tag{6}$$

Where, R (■) is a unit step function which can be represented by $\mathbb{R}(i) = \begin{cases} 1, & i \succcurlyeq 0 \\ 0, & i \prec 0 \end{cases}$

Here, consider spatial image field can be represented as λ and artifacts present in the available *dermoscopic* images is denoted as $b(y): \lambda \to Z$, undetermined bias area in the *dermoscopic* image is expressed as $X(y): \lambda \to Z$ and At the end, reconstructed original image signal is indicated as $K(y): \lambda \to Z$ then color pixel difference in *dermoscopic* images is given by,

$$M(y) = X(y).K(y) + b(y) \tag{7}$$

Consider, spatial image field λ consists of G number of entities then spatial image field of d^{th} entity is denoted by λ_d. Consider that for each entity, reconstructed original image signal $K(y)$ is expressed as a piece wise constant i.e. $K(y) = f_d$ where y belongs to all values of λ_d and f_d behaves as a constant that represents the color variation feature of the a^{th} entity. The undetermined bias area in *dermoscopic* images helps to find out proper boundaries of spatial image fields λ and works as a smooth function. The artifacts present in the *dermoscopic* images are Gaussian type whose mean and variance parameters can be denoted as Ω_d and ${\delta_d}^2$ correspondingly. Here, mean parameter is taken as zero. Moreover, the color pixels of the spatial image field λ can be estimated with the help of mean and variance parameters whereas Contour features of pixel color can be determined using Gaussian samples. However, several Gaussian samples are required to achieve high quality image segmentation. Moreover, for each entity field one Gaussian sample is considered to evaluate Contour features. Then, the Gaussian sample for their corresponding entity field λ_d can be represented in the following equation as,

$$h(M(c)(\psi_d) = \frac{1}{\left(\left((2\pi)^{1/2}\right).\delta_d\right)} e^{-(M(c)-\Omega_d(y))^2.\left(2\delta_d^2\right)^{-1}} \tag{8}$$

Where, $M(c)$ is the image under consideration and ψ_d is used to represent features of the a^{th} entity and variance deviation is denoted as δ_d and diversified mean is expressed as $\Omega_d(y)$. Consider, undetermined bias area $X(y)$ in the *dermoscopic* image as zero as it shows very less variations and can be represented as,

$$\Omega_d(y) \cong X(y).f_d \tag{9}$$

Here, ψ_d is indicated as $\psi_d = \{f_d, \delta_d, X\}$ and the adjacent central field of spatial image field λ for each y is given as,

$$R_y = \{c \| \|c - y\| \leq \mu\} \tag{10}$$

Where, Equation (10) represents small neighbourhood. Maximum neighbourhood considered is equal to the radius of the entity and radius of adjacent central field R_y of spatial image field λ can be denoted as h. Here, the number of non-overlapping entities are available in the input image $M(y)$ is G whose spatial image field of d^{th} entity is denoted by λ_d. Then, the full set of spatial image field λ can be determined as,

$$\lambda = {}_{d=1,\ldots,G}\lambda_d \tag{11}$$

Here, λ_d and λ_a intersection gives the value of Φ where for all values $d \neq a$. Where, d and a are two entities. The reconstructed color pixel region $L(E)$ can be transformed into another domain say $Z(E)$ by using mapping methods and determined by Equation (12),

$$E : M(y|\psi_d) \to T(y|\psi_d) \tag{12}$$

Here, Equation (12) is further simplified by the following step,

$$T(y|\psi_d) = 1/q_d(y) \sum_{c \in \lambda_d \cap R_y} M(c|\psi_d) \tag{13}$$

Moreover, color of pixels is autonomously dispersed throughout the image and their dispersion can be shown by y hence $q_d(y) = \lambda_d \cap R_y$. Then, the relative density of continuous random color pixels is recognized as Gaussian type for each $T(y|\psi_d) \in Z(E)$ and can be expressed as,

$$T(y|\psi_d) = G\left(\Omega_d, \frac{\delta_d^2}{q_d(y)}\right) \tag{14}$$

Consider that product of each relative density of continuous random color pixels still recognized as Gaussian type as shown in Equation (15),

$$M(c|\psi_d) \cong M(c|\psi_d) \tag{15}$$

Here, the intersection of λ_d and R_y corresponds to all values of c. Then, the Gaussian function for relative density of continuous random color pixels is defined by the following Equation (16),

$$\prod_{c\varepsilon\, \lambda_d \cap R_y} h\left(M\left(c(\psi_d)\right)\right) = h\left(M\left(y(\psi_d)\right)^{q_d(y)}\right) \tag{16}$$

Here, from Equation (14) it is evident that both Gaussian distribution function then $\prod_{c\varepsilon\, \lambda_d \cap R_y} h\left(M\left(c(\psi_d)\right)\right)$ is directly proportional to $G\left(\Omega_d,\ \delta_d^2.\ \left(q_d(y)\right)^{-1}\right)$. Therefore,

$$h\left(T\left(y(\psi_d)\right)\right) = \prod_{c\varepsilon\, \lambda_d \cap R_y} h\left(M\left(c(\psi_d)\right)\right) \tag{17}$$

Consider that,

$$L = \left\{T\left(y(\psi_d)\right),\ y\ \varepsilon\ \lambda,\ \ d = 1,2,3\ldots..,G\right\} \tag{18}$$

Here, L is a variable representing d^{th} entity. Then, relative density of continuous random color pixels of the d^{th} entity is defined as,

$$h\left(L\left(\psi_d\right) = \prod_{y\,\in\,\lambda} h\left(T\left(y(\psi_d)\right)\right)\right. \tag{19}$$

Then, the reconstructed joint relative density of continuous random color pixels is determined with the help of proposed Adaptive Contour Model (ACM) for *dermoscopic* image segmentation as,

$$h\left(L\left(\Psi\right) = \prod_{d=1}^{G} h\left(L\left(\psi_d\right)\right)\right. \tag{20}$$

Here, Equation (20) can be further simplified in Equations (21) and (22) and is defined as follows,

$$h\left(L(\Psi) = \prod_{d=1}^{G}\prod_{y\,\in\,\lambda} h\left(\left(T\left(y(\psi_d)\right)\right)\right)\right. \tag{21}$$

$$h\left(L(\Psi) = \prod_{y\,\in\,\lambda} n\left(T\left(y(\Psi)\right)\right)\right. \tag{22}$$

Where, $\Psi = \left\{\psi_d,\ d = 1,2,..,G\right\}$. And $\prod_{d=1}^{G} h = n$ then

$$n\left(T\left(y(\Psi)\right)\right) = \prod_{d=1}^{G} h\left(T\left(y(\psi_d)\right)\right) \tag{23}$$

Here, Equation (23) is further simplified as follows,

$$n\left(T\left(y(\Psi)\right)\right) = \prod_{d=1}^{G}\prod_{c\varepsilon\, \lambda_d \cap R_y} h\left(M\left(c(\psi_d)\right)\right) \tag{24}$$

With the help of Equations (16) and (24), the dispersion of covariate Gaussian samples is obtained as follows,

$$n\left(\left(T\left(y(\Psi)\right)\right)\right) = \prod_{d=1}^{G} h\left(T\left(y(\psi_d)\right)\right) \propto G\ (\Omega, \varphi\ ) \tag{25}$$

Here, $h\left(T\left(y(\psi_d)\right)\right)$ is directly proportional to $G\ (\Omega,\ \varphi)$ and Ω is defined by $\varphi\ .\sum_{d=1}^{G} q_d(y).\ \frac{\Omega_d}{\left(\delta_d^2\right)}$ and φ is defined by $\frac{1}{\sum_{d=1}^{G} q_d(y).\ \left(\delta_d^2\right)^{-1}}$.

Moreover, the logarithm energy function $k(\Psi)$ can be represented with respect to $h(L|\Psi)$ as shown in Equation (22),

$$k(\Psi) \triangleq\ -logh(L|\Psi) \tag{26}$$

Here, Equation (26) can be further simplified by following equation,

$$k(\Psi)\ \triangleq\ p - \sum_{d=1}^{G}\int_{\lambda}\int_{\lambda_d \cap R_y} log\left(h\left(M\left(c(\psi_d)\right)\right)\right).\, dy.dx \tag{27}$$

Here, p is a constant parameter and Assume that, for the area R_y in the image field λ , $\chi_\mu\,(y,c)$ defines as a measure function and expressed by the following equation,

$$\chi_\mu\,(y,c) = \begin{cases} 1, & \|c-y\| \preccurlyeq \mu \\ 0, & else \end{cases} \tag{28}$$

From Equations (8) and (29), the constant parameter p can be removed and logarithm energy function $k\,(\Psi)$ is redefined as,

$$k\,(\Psi) = \sum_{d=1}^{G} \int_\lambda \int_{\lambda_d} \chi_\mu\,(y,c) \left[log\,(\delta_d) + \left\{ (M\,(c) - X\,(y)\,f_d)^2 \right\} . \left(2\delta_d^2\right)^{-1} \right] \tag{29}$$

Here, reconstructed joint relative density of continuous random color pixels is expressed by the above Equation (22) which gives information about pixel structure and pixel color of various contour classes. From the Equation (13), it is observed that the reconstructed color pixel region can be transferred to another image field of similar color pixel region. Thus, the proposed model provides output without any artifacts and hence the quality of segmentation remains very high and sharp edges can be obtained while segmentation of *dermoscopic* images.

3 Results and Discussion

Contour feature extraction and lesion edge detection provide proficient segmented output result with sharp boundaries. Gaussian Artifacts are removed using pre-processing methods. The proposed Active Contour Model (ACM) is compared with various recent state-of-art-segmentation-techniques for Melanoma detection in order to validate the robustness and high efficiency of the proposed ACM. The Segmentation of *Dermoscopic* images using proposed Adaptive Contour Model (ACM) is achieved with 64-bit Windows 10 OS and intel core processor with 16 *GigaBytes* (GB) RAM. The comparative analysis of proposed Adaptive Contour model is presented with the help of segmentation performance evaluation matrices which are *Jaccard* index (JA), Dice coefficient (DI) and accuracy (AC). This evaluation matrix can be defined by the following equations as,

$$JA = |t_{rp}| \,.\, \left[|t_{rp}| + |f_{sp}| + |f_{sn}| \right]^{-1} \tag{30}$$

$$AC = \left[|t_{rp}| + |t_{rn}| \right] .\, \left[|t_{rp}| + |t_{rn}| + |f_{sp}| + |f_{sn}| \right]^{-1} \tag{31}$$

$$DI = \left[2 \times |t_{rp}| \right] .\, \left[2 \times |t_{rp}| + |f_{sp}| + |f_{sn}| \right]^{-1} \tag{32}$$

Where, t_{rn} represent true negative values, t_{rp} represents true positive values. Similarly, f_{sn} represents false negative values and f_{sp} represents false positive values.

3.1 Segmentation Quality Comparison

This section discusses about the quality of segmentation using the proposed Active Contour Model (ACM) over PH2 and ISIC Challenge 2017 *Dermoscopic* images. All the 200 *Dermoscopic* images present in the PH2 dataset is tested using proposed ACM and segmentation quality is evaluated based on *Jaccard* index (JA), Dice coefficient (DI) and accuracy (AC) matrices. The robustness of the proposed ACM is validated for PH2 dataset by comparing segmentation results with various state-of-art-techniques. The quantitative performance of PH2 dataset is presented in and the qualitative performance of PH2 dataset is shown in Figure 1**(a –c row)**. All the three segmentation evaluation matrices show significant improvement. The quantitative performance of PH2 dataset is compared with recent state-of-art-techniques like, *Peng et. al.*[18], *Xie et. al.*[19], *Goyal et. al.* [20], *iMSCGnet* [21] and qualitative performance of PH2 dataset is compared with different applications of *iMSCGnet* [21] Segmentation technique as shown in Figure 1 **(a –c row)**. The performance results are highly superior to any other state-of-art-techniques using proposed ACM for PH2 dataset. The performance matrices indicate high quality of segmentation process. Thus, the performance indices are such as *Jaccard* index (JA) is 89.14, Dice coefficient (DI) is 93.98 and accuracy (AC) is 96.95 which is better considering PH2 dataset.

Similarly, all the 600 *Dermoscopic* images present in the ISIC Challenge 2017 dataset is tested using proposed ACM. Moreover, the proposed ACM outperforms state-of-art-techniques in terms of *Jaccard* index (JA), Dice coefficient (DI) and

accuracy (AC) matrices. The robustness of the proposed ACM is validated for ISIC Challenge 2017 dataset by comparing segmentation results with various state-of-art-techniques. The quantitative performance of ISIC Challenge 2017 dataset is presented in Table 2 and the qualitative performance of ISIC Challenge 2017 dataset is shown in Figure 1**(d-f)** and Figure 2. The quantitative performance of ISIC dataset is compared with recent state-of-art-techniques like, *FocusNet* [22], *Lie et. al.* [23], *PA – Net* [24], *iMSCGnet* [21] and qualitative performance of ISIC dataset is compared with different applications of *iMSCGnet* [21] Segmentation technique as shown in Figure 1 **(a –c row)** and Figure 2. The quality of segmentation images is very similar to the Ground Truth (GT) images due to accurate contour feature extraction and edge detection using proposed Adaptive Contour Model (ACM). All the three segmentation evaluation matrices show significant improvement. This validates that the proposed ACM will be very significant for various medical applications. The performance results are highly superior to any other state-of-art-techniques using proposed ACM for ISIC Challenge 2017 dataset. The performance matrices indicate high quality of segmentation process. Thus, the performance indices are such as *Jaccard* index (JA) is **79.23**, Dice coefficient (DI) is **87.26** and accuracy (AC) is **94.63** which is quite high considering ISIC dataset. Figure 3 represents Segmentation results Comparison of proposed ACM with State-of-art-techniques considering ISIC dataset

Table 1. Comparison of proposed ACM with other methods over PH2 dataset

Methods	*Jaccard Index (JA)*	Dice Coefficient	Accuracy (AC)
Peng et. al. [18]	85.00	90.00	93.00
Xie et. al. [19]	85.70	91.90	94.90
Goyal et. al. [20]	83.90	90.70	93.80
iMSCGnet [21]	88.21	93.36	95.71
Ours (ACM)	89.14	93.98	96.95

Table 2. Comparison of proposed ACM with other methods over ISIC dataset

Methods	*Jaccard (JA)*	Dice Coefficient	Accuracy (AC)
FocusNet [22]	75.62	83.15	92.14
Lie et. al. [23]	76.50	86.60	93.90
PA – Net [24]	77.60	85.80	93.60
iMSCGnet [21]	77.60	85.83	93.58
Ours (ACM)	79.23	87.26	94.63

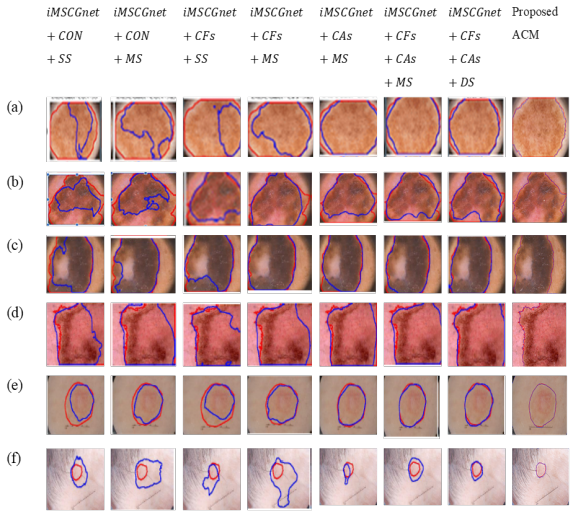

Fig 1. Qualitative Comparison of proposed ACM with applications over two datasets. The samples in row (a-c) and row (d-f) are from PH2 and ISICI2017, respectively. Red and blue contours are ground truths and segmentation Outcomes, separately

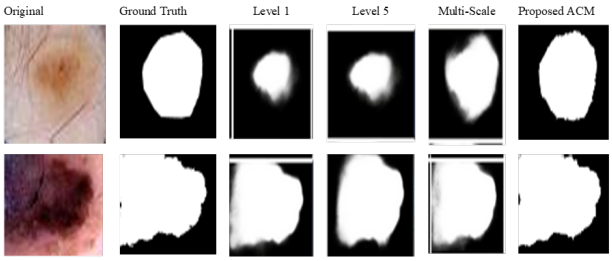

Fig 2. Segmentation results Comparison of proposed ACM with applications of *iMSCGnet* Algorithm considering ISIC dataset

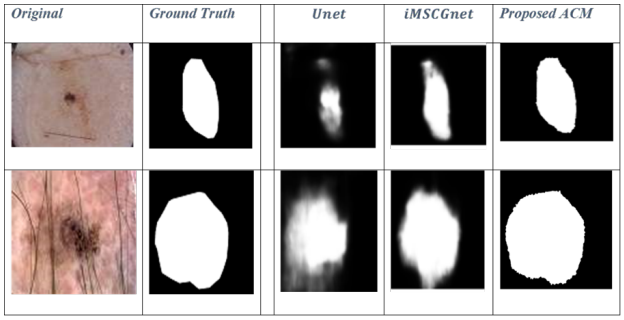

Fig 3. Segmentation results Comparison of proposed ACM with State-of-art-techniques considering ISIC dataset

4 Conclusion

Melanoma skin cancer disease detection in preliminary stages can save thousands of life every year due to its high mortality rate in advanced stages. Therefore, an efficient lesion segmentation method is realized for the detection of Melanoma skin cancer disease at preliminary stages and timely comprehensive assessment of Melanoma disease based on Active Contour Model (ACM). High quality segmentation is achieved based on contour features and sharp edge detection using ACM. Probability function is utilized for color pixel transformation from one domain to another in its neighbouring area.

Gaussian noise present in *Dermoscopic* images is removed using pre-processing methods. A comprehensive mathematical representation is presented for Gaussian noise removal, contour feature extraction and accurate edge detection to enhance segmentation quality. The robustness of the proposed ACM is validated for PH2 dataset and ISIC Challenge 2017 dataset in comparison with various state-of-art-techniques. The quantitative and qualitative performance evaluation of PH2 dataset and ISIC Challenge 2017 is shown in comparison with various state-of-art-techniques considering performance matrices like *Jaccard* index (JA), Dice coefficient (DI) and accuracy (AC). The performance indices are such as *Jaccard* index (JA) is **89.14**, Dice coefficient (DI) is 93.98 and accuracy (AC) is **96.95** which is quite high considering PH2 dataset. Similarly, *Jaccard* index (JA) is **79.23**, Dice coefficient (DI) is **87.26** and accuracy (AC) is **94.63** which is also quite high considering ISIC dataset. Therefore, the performance matrices indicate high quality of segmentation process and can be utilized in several medical applications. Every research work has its own advantages and limitations. However, the main cause for limited results can be improper removal of artifacts or improper training or inadequate resources or inaccurate modeling of the proposed model, etc. This can be further improved with advanced methods for removal of artifacts.

References

1) Pham TC, Tran GS, Nghiem TP, Doucet A, Luong CM, Van-Dung Hoang. A Comparative Study for Classification of Skin Cancer. In: 2019 International Conference on System Science and Engineering (ICSSE). IEEE. 2019;p. 267–272. Available from: https://ieeexplore.ieee.org/document/8823124.
2) Cancer Statistics Center. 2019. Available from: https://cancerstatisticscenter.cancer.org.
3) Jana E, Subban R, Saraswathi S. Research on Skin Cancer Cell Detection Using Image Processing. In: 2017 IEEE International Conference on Computational Intelligence and Computing Research (ICCIC). IEEE. 2018;p. 1–8. Available from: https://ieeexplore.ieee.org/document/8524554.

4) Jooravan A, Reddy S, Pillay N. Comparative Study of Binary Classifiers for Reducing False Negative Detection of Melanoma in Skin Lesions. In: 2022 International Conference on Engineering and Emerging Technologies (ICEET). IEEE. 2023;p. 1–6. Available from: https://ieeexplore.ieee.org/document/10007359.
5) Tanwar, & Raman V, & Balasubramanian, Rajput, Bhargava R. CryptoLesion: A Privacy-preserving Model for Lesion Segmentation Using Whale Optimization over Cloud. *ACM Transactions on Multimedia Computing, Communications, and Applications*. 2020;16(2):1–23. Available from: https://doi.org/10.1145/3380743.
6) Ünver HM, Ayan E. Skin Lesion Segmentation in Dermoscopic Images with Combination of YOLO and GrabCut Algorithm. *Diagnostics*. 2019;9(3):1–21. Available from: https://doi.org/10.3390/diagnostics9030072.
7) Xie Y, Zhang J, Xia Y, Shen C. A Mutual Bootstrapping Model for Automated Skin Lesion Segmentation and Classification. *IEEE Transactions on Medical Imaging*. 2020;39(7):2482–2493. Available from: https://ieeexplore.ieee.org/document/8990108.
8) Wei Z, Song H, Chen L, Li Q, Han G. Attention-Based DenseUnet Network With Adversarial Training for Skin Lesion Segmentation. *IEEE Access*. 2019;7:136616–136629. Available from: https://ieeexplore.ieee.org/document/8835031.
9) Khan MQ, Hussain A, Rehman SU, Khan U, Maqsood M, Mehmood K, et al. Classification of Melanoma and Nevus in Digital Images for Diagnosis of Skin Cancer. *IEEE Access*. 2019;7:90132–90144. Available from: https://ieeexplore.ieee.org/document/8756036/authors#authors.
10) Goyal M, Oakley A, Bansal P, Dancey D, Yap MH. Skin Lesion Segmentation in Dermoscopic Images With Ensemble Deep Learning Methods. *IEEE Access*. 2019;8:4171–4181. Available from: https://ieeexplore.ieee.org/document/8936444.
11) Wang X, Jiang X, Ding H, Liu J. Bi-Directional Dermoscopic Feature Learning and Multi-Scale Consistent Decision Fusion for Skin Lesion Segmentation. *IEEE Transactions on Image Processing*. 2019;29:3039–3051. Available from: https://ieeexplore.ieee.org/document/8917805?denied=.
12) Berkay M, Mergen EH, Binici RC, Bayhan Y, Gungor A, Okur E, et al. Deep Learning based Melanoma Detection from Dermoscopic Images. In: 2019 Scientific Meeting on Electrical-Electronics & Biomedical Engineering and Computer Science (EBBT). IEEE. 2019;p. 1–4. Available from: https://ieeexplore.ieee.org/document/8741934/authors#authors.
13) Wei L, Ding K, Hu H. Automatic Skin Cancer Detection in Dermoscopy Images Based on Ensemble Lightweight Deep Learning Network. *IEEE Access*. 2020;8:99633–99647. Available from: https://ieeexplore.ieee.org/document/9099799.
14) Gessert N, Sentker T, Madesta F, Schmitz R, Kniep H, Baltruschat I, et al. Skin Lesion Classification Using CNNs With Patch-Based Attention and Diagnosis-Guided Loss Weighting. *IEEE Transactions on Biomedical Engineering*. 2020;67(2):495–503. Available from: https://ieeexplore.ieee.org/document/8710336.
15) Ali AR, Li J, O'shea SJ. Towards the automatic detection of skin lesion shape asymmetry, color variegation and diameter in dermoscopic images. *PLOS ONE*. 2020;15(6):1–21. Available from: https://doi.org/10.1371/journal.pone.0234352.
16) Yang C, Wu L, Chen Y, Wang G, Weng G. An Active Contour Model Based on Retinex and Pre-Fitting Reflectance for Fast Image Segmentation. *Symmetry*. 2022;14(11):1–25. Available from: https://doi.org/10.3390/sym14112343.
17) Fang L, Wang X, Zhao M. Integrated vector-valued active contour model for image segmentation. *Signal, Image and Video Processing*. 2022;16(1):193–201. Available from: https://doi.org/10.1007/s11760-021-01979-2.
18) Peng Y, Wang N, Wang Y, Wang M. Segmentation of dermoscopy image using adversarial networks. *Multimedia Tools and Applications*. 2019;78(8):10965–10981. Available from: https://doi.org/10.1007/s11042-018-6523-2.
19) Xie F, Yang J, Liu J, Jiang Z, Zheng Y, Wang Y. Skin lesion segmentation using high-resolution convolutional neural network. *Computer Methods and Programs in Biomedicine*. 2020;186:105241. Available from: https://doi.org/10.1016/j.cmpb.2019.105241.
20) Goyal M, Oakley A, Bansal P, Dancey D, Yap MH. Skin Lesion Segmentation in Dermoscopic Images With Ensemble Deep Learning Methods. *IEEE Access*. 2019;8:4171–4181. Available from: https://ieeexplore.ieee.org/document/8936444.
21) Tang Y, Fang Z, Yuan S, Zhan C, Xing Y, Zhou JT, et al. iMSCGnet: Iterative Multi-Scale Context-Guided Segmentation of Skin Lesion in Dermoscopic Images. *IEEE Access*. 2020;8:39700–39712. Available from: https://ieeexplore.ieee.org/document/9007375.
22) Kaul C, Manandhar S, Pears N. Focusnet: An Attention-Based Fully Convolutional Network for Medical Image Segmentation. In: 2019 IEEE 16th International Symposium on Biomedical Imaging (ISBI 2019). IEEE. 2019;p. 455–458. Available from: https://ieeexplore.ieee.org/document/8759477.
23) Li H, He X, Zhou F, Yu Z, Ni D, Chen S, et al. Dense Deconvolutional Network for Skin Lesion Segmentation. *IEEE Journal of Biomedical and Health Informatics*. 2019;23(2):527–537. Available from: https://ieeexplore.ieee.org/document/8419237.
24) Wang H, Wang G, Sheng Z, Zhang S. Automated Segmentation of Skin Lesion Based on Pyramid Attention Network. In: International Workshop on Machine Learning in Medical Imaging, MLMI 2019;vol. 11861 of Lecture Notes in Computer Science. Springer, Cham. 2019;p. 435–443. Available from: https://doi.org/10.1007/978-3-030-32692-0_50.